JOURNAL OF CHEMICAL EDUCATION

pubs.acs.org/jchemeduc Article

Structure Analysis from Powder Diffraction Data: Rietveld Refinement in Excel

John S. O. Evans* and Ivana Radosavljevic Evans

Cite This: *J. Chem. Educ.* 2021, 98, 495−505 Read Online

ACCESS | Metrics & More | Article Recommendations | Supporting Information

ABSTRACT: Powder diffraction is one of the most widely used analytical techniques for characterizing solid state materials. It can be used for phase or polymorph identification, quantitative analysis, cell parameter determination, or even full crystal structure analysis using the powerful Rietveld refinement method. As with much of modern crystallography, the software used for Rietveld refinement is frequently treated as a "black box" that produces often poorly understood outputs. This paper shows how it is possible for students to perform a full Rietveld refinement against experimental powder diffraction data from scratch using a simple spreadsheet like Excel. It starts by reviewing the basic ideas of least-squares fitting a straight line, develops these into fitting simple functions to peaks in simulated experimental data, and then combines these ideas with crystallographic equations to enable Rietveld refinement of the structure of an inorganic material (rutile, TiO_2). At each stage, students can self-learn different fundamental aspects and pitfalls of data analysis that are widely reapplicable. The ideas can be taught as an online learning exercise or could be incorporated in a laboratory class where students collect and analyze their own experimental data.

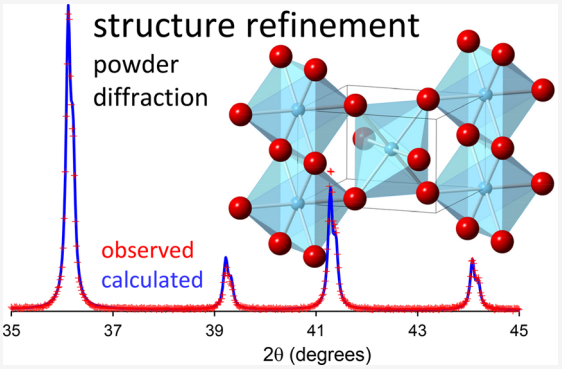

KEYWORDS: *Upper-Division Undergraduate, Graduate Education/Research, Laboratory Instruction, Computer-Based Learning, Materials Science, Solid State Chemistry, Inorganic Chemistry, Physical Chemistry, X-ray Crystallography*

Downloaded via CHALMERS UNIV OF TECHNOLOGY on March 25, 2024 at 16:14:27 (UTC).
See https://pubs.acs.org/sharingguidelines for options on how to legitimately share published articles.

1. INTRODUCTION

X-ray and neutron diffraction are among the most powerful analytical techniques for probing chemical structure in the solid state, and they are widely used in academic, industrial, and environmental research ranging from the fundamental to the applied. The breadth and importance of the techniques are exemplified by the Cambridge Structural Database, which contains over 1,000,000 organic/organometallic entries that have been crystallographically characterized;[1] the ICSD which contains over 200,000 inorganic crystal structure;[2] and the International Centre for Diffraction Data's Powder Diffraction File PDF-4,[3] which contains over 425,000 inorganic entries. As such, the fundamentals of crystallography are taught in many undergraduate chemistry, physics, engineering, materials, pharmaceutical science, and life science courses. One of the challenges in inspiring students about crystallographic methods is that the data analysis required to go from experimental data to a final structural model relies on sophisticated and specialized software that has a steep learning curve. The result is that such software is often treated by users as a black box. It also leads to significant gaps developing between the theory students see in lectures and textbooks, and the way they experience crystallography in a practical setting. Several publications have previously raised the educational consequences, and there have been a number of earlier papers on how to build crystallographic education into school, undergraduate and postgraduate, curricula.[4−15] Several previous publications have described ways in which powder diffraction experiments can be introduced into undergraduate practical classes to highlight the importance of the technique itself,[6,16−18] or its use as a characterization method as part of a wider laboratory practical.[19−23] We are, however, unaware of other work that teaches structure analysis from powder diffraction data in the way described here.

The paper is based on a training exercise we have run in graduate-level schools over the past 10 years, but it is equally appropriate for advanced undergraduate students. It guides students from the very general ideas of data analysis to the point where they can perform a full Rietveld structural analysis on a simple material using nothing more than Microsoft Excel's built-in "Solver" function. By working from experimental data right through to a three-dimensional structure, students learn many of the key aspects of crystallographic analysis, as well as

Received: July 30, 2020
Revised: November 5, 2020
Published: November 25, 2020

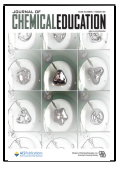

ACS Publications

© 2020 American Chemical Society and Division of Chemical Education, Inc.

https://dx.doi.org/10.1021/acs.jchemed.0c01016
J. Chem. Educ. 2021, 98, 495−505

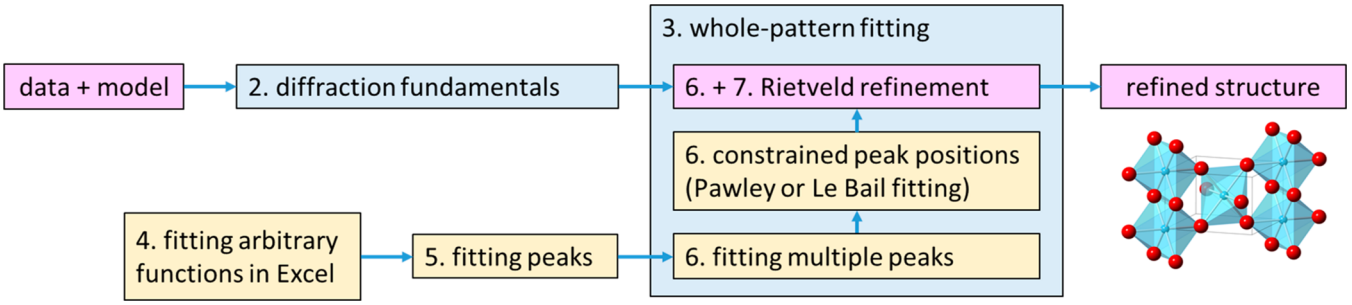

Figure 1. Schematic of how the different sections of the paper interact: the background theory in Sections 2 and 3 (shaded blue) allows students to build-up the complexity of data analysis through Sections 4, 5, and 6 (yellow boxes); they can then achieve the goal of going directly from experimental data and a model structure to a final Rietveld-refined structure (pink boxes).

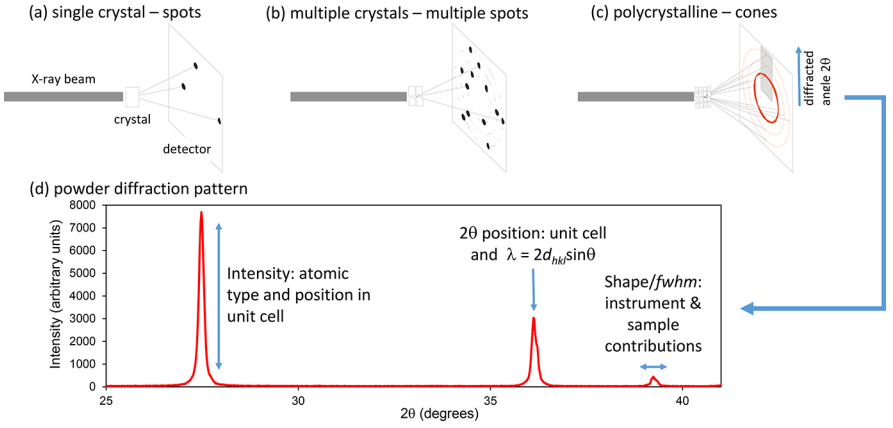

Figure 2. (a) A single crystal gives rise to diffracted beams in discrete directions which appear as "spots" on a 2D detector. (b) With multiple crystals, spots will be seen from each crystal. (c) In a powdered or polycrystalline sample, this leads to cones of diffracted intensity which are intersected as circles on a 2D detector, with each circle corresponding to an individual or overlapped set of *hkl* reflections. A one-dimensional scan in 2θ across these rings (or integration around them) leads to (d) a powder diffraction pattern as a plot of diffracted intensity as a function of angle 2θ.

least-squares fitting skills that are widely reapplicable in other areas. By performing all steps in the data analysis from the bottom-up, they learn through experience how crystallographic refinements work, and how they can fail. As such, we hope that the paper will help address many of the educational issues outlined in the previous paragraph.

The paper is organized into eight main sections (see Figure 1) allowing instructors to tailor training depending on the students' backgrounds and the time available. Section 2 gives a brief overview of diffraction and includes the important equations that are used in later data analysis. Section 3 describes the ideas behind whole-powder-diffraction-pattern fitting methods such as Rietveld and Pawley/Le Bail refinement.[24−26] These sections contain the background information students need to understand the work, or that nonspecialist teaching assistants (TAs) will need to support student learning. Section 4 gives a very basic introduction to least-squares fitting using Excel's Solver function and then explores fitting either linear or nonlinear functions to experimental data. Section 5 takes the ideas of data fitting and develops them into fitting experimental peaks using the commonly used Gaussian or Lorentzian functions. Section 6 then explores how to fit multiple peaks in a data set at either freely refined positions or, as in powder diffraction analysis, at positions determined by the size and shape of a unit cell. We then introduce the constraint that the peak intensities are determined by the types of atoms and their positions in the unit cell, allowing a structural model to be least-squares fitted to an experimental data set: Rietveld refinement. Since Rietveld refinement is the ultimate goal of the paper, it is treated in the most detail, and students could choose to skip the earlier parts of Section 6. Section 7 allows students to perform a Rietveld refinement on real experimental data, either provided in the accompanying Excel spreadsheet, or that they collect themselves. Finally, Section 8 summarizes our learning from using these exercises in a classroom setting and our assessment of their effectiveness.

We have tried to include sufficient information such that the sections of the paper targeted at students can be read as a stand-alone manuscript and have kept the paper's mathematical and crystallographic content at the minimum level we believe is needed for students to understand the process. We are aware that we have omitted many important details for brevity, so we provide references to more detailed texts where appropriate.

We have provided an Excel spreadsheet as Supporting Information which contains all the data, instructions, and equations needed to work through each example, and which contains "pop-up help boxes" for students. We have also provided instructor/TA notes in the Supporting Information which outline the tasks students could follow, sets "challenge questions", and suggests discussion points at different stages. Corresponding step-by-step tutorials are available online.[27] We also provide example data files so students could repeat this

https://dx.doi.org/10.1021/acs.jchemed.0c01016
J. Chem. Educ. 2021, 98, 495−505

analysis in widely used specialist software packages for Rietveld refinement.

2. DIFFRACTION FUNDAMENTALS

When electromagnetic radiation with a wavelength comparable to interatomic separations is incident on a crystalline sample, each atom acts as a source of scattered radiation and the constructive/destructive interference between the scattered waves leads to diffraction. If we picture a crystal as containing planes described by Miller indices (hkl), Bragg's law gives the angle of constructively scattered intensity via

$$\lambda = 2d_{hkl} \sin\theta \tag{1}$$

where λ is the wavelength, d_{hkl} the interplanar spacing, and 2θ the direction relative to the incident beam. For any crystal system, d_{hkl} can be related to the unit-cell parameters a, b, c, α, β, γ by trigonometry. For a tetragonal unit cell ($a = b \neq c$; $\alpha = \beta = \gamma = 90°$), the general expression simplifies to

$$\frac{1}{d_{hkl}^2} = \frac{h^2 + k^2}{a^2} + \frac{l^2}{c^2} \tag{2}$$

Equations 1 and 2 tell us that the possible angles of diffracted intensity ($2\theta_{hkl}$) in any diffraction pattern depend solely on the size and shape of the unit cell. For a single crystal, we get beams of diffracted intensity in specific directions when Bragg's law is satisfied. For a polycrystalline material, the random orientation of crystallites (Figure 2) means that these beams become averaged into concentric cones. In a traditional powder diffraction experiment, a detector is scanned across these cones to produce a plot of diffracted intensity versus angle 2θ: a powder diffraction pattern. For data analysis, patterns are normally treated as a series of $y_{obs,i}$ intensity values at N discrete 2θ steps.

The intensity I_{hkl} of each hkl reflection is determined by the identity and positions of the atoms inside the unit cell via the structure factor, F_{hkl}:

$$F_{hkl} = \sum_j t_j f_j \exp[2\pi i(hx_j + ky_j + lz_j)] \tag{3}$$

$$I_{hkl} \propto |F_{hkl}|^2 \tag{4}$$

Here, x_j, y_j, and z_j are fractional atomic coordinates of atom j, and f_j describes the scattering factor of atom j as a function of $\sin\theta/\lambda$. The t_j term accounts for the fact that atoms vibrate around their average positions in real samples, which decreases I_{hkl} intensities. In this paper, we will use an isotropic correction $t_j = \exp(-B \sin^2\theta/\lambda^2)$, where the atomic displacement parameter B (the "temperature factor" or "Debye–Waller" factor) is expressed as $B = 8\pi^2u^2$, and u is the root mean squared atomic displacement in Å. It is worth noting that this parameter is typically poorly determined from laboratory powder X-ray data; over a short 2θ range, B correlates highly with the overall scale factor and can be strongly affected by factors such as the sample absorption and any surface roughness in a reflection geometry experiment.

For a powder diffraction experiment, several factors usually appear in the $I_{hkl} \propto |F_{hkl}|^2$ proportionality constant: an overall scale factor, factors describing the diffractometer geometry in the so-called LP or Lorentz polarization factor, and the reflection multiplicity m. m counts the number of symmetry equivalent reflections for each hkl. For example, in a tetragonal system, the (110) reflection has multiplicity 4 [(110), $(\bar{1}10)$, $(\bar{1}\bar{1}0)$, $(1\bar{1}0)$]. All of these terms are described in full detail in most crystallography texts.[24,28−30]

In this paper, we ultimately explore the example of rutile TiO_2, using diffraction data recorded on a powder diffractometer with Cu Kα radiation produced by a graphite monochromator set at an angle ($2\theta_{mono}$) of 26.6°. Rutile is tetragonal, has the space group $P4_2/mnm$, has $a \approx 4.6$ Å and $c \approx 2.96$ Å, and contains Ti on Wyckoff site 2a (0, 0, 0) [symmetry generates a second atom at (1/2, 1/2, 1/2)] and an oxygen on 4f (x, x, 0) with $x \approx 0.3$ [symmetry generates ($-x$, $-x$, 0), ($-x + 1/2$, $x + 1/2$, 1/2), ($x + 1/2$, $-x + 1/2$, 1/2); $x = 0.30631$ was used for simulated data sets]. For this example, the intensity of each hkl reflection[31] can be calculated using the following equations:

$$I_{hkl} = \text{scale} \times \text{LP} \times m \times F_{hkl}^2 \tag{5}$$

$$F_{hkl} = t_{Ti} f_{Ti} A_{Ti} + t_O f_O A_O \tag{6}$$

$$A_{Ti} = 2\cos^2 2\pi\left(\frac{h + k + l}{4}\right) \tag{7}$$

$$A_O = 2\cos 2\pi lz\left[\cos 2\pi\left(hx - \frac{h + k + l}{4}\right) \cos 2\pi\left(ky + \frac{h + k + l}{4}\right)\cos 2\pi\left(kx - \frac{h + k + l}{4}\right) \cos 2\pi\left(hy + \frac{h + k + l}{4}\right)\right] \tag{8}$$

$$t_j = \exp\left(\frac{-B_j \sin^2\theta}{\lambda^2}\right) \tag{9}$$

$$\text{LP} = \frac{1 + \cos^2 2\theta_{mono} \cos^2 2\theta}{\sin^2\theta \cos\theta} \qquad 2\theta_{mono} = 26.6° \tag{10}$$

Equations 6−8 are a simplification of the more general eq 3 for this specific structure, and they allow us to use just the symmetry-unique atoms in calculations.

In any real diffraction experiment, each hkl reflection is observed over a small range of 2θ values giving a peak of finite width. The shape of the peak is caused by a combination (strictly a convolution) of effects from the radiation source, the diffractometer components, and the sample.[24] While the details of peak shape can be of enormous scientific importance, we will just take an empirical approach and state that peaks can often be described analytically by either Gaussian or Lorentzian functions, or by some combination of the two (e.g., a Voigt or pseudo-Voigt function). For this paper, we adopt the unit area peak shape definitions given by Young:[26]

$$G = \frac{C_0^{1/2}}{fwhm \cdot \pi^{1/2}} \exp\left(\frac{-C_0(2\theta - 2\theta_{hkl})^2}{fwhm^2}\right) \tag{11}$$

$$L = \frac{C_1^{1/2}}{fwhm \cdot \pi} 1/\left[1 + C_1\frac{(2\theta - 2\theta_{hkl})^2}{fwhm^2}\right] \tag{12}$$

$$pV = \eta L + (1 - \eta)G \tag{13}$$

where $C_0 = 4 \ln 2$, $C_1 = 4$, 2θ is the diffraction angle in question, $2\theta_{hkl}$ is the peak position, and η is a mixing

https://dx.doi.org/10.1021/acs.jchemed.0c01016
J. Chem. Educ. 2021, 98, 495−505

parameter. The peak full-width at half-maximum ($fwhm$) usually varies smoothly with 2θ.

3. WHOLE-POWDER-PATTERN FITTING AND RIETVELD REFINEMENT

While single crystal diffraction is considered the gold standard for determination of crystal structures, powder diffraction has many of its own distinct advantages: for many compounds, it can be difficult or impossible to grow diffraction-quality single crystals; samples can be readily studied under real working conditions (e.g., *operando* catalysis/batteries); samples can be studied through phase transitions where single crystals would be destroyed; and multiphase samples can be studied allowing qualitative or quantitative phase analysis.[32] For these reasons, powder diffraction[33,34] has often provided the crucial breakthrough structural insights in diverse areas such as high-temperature superconductors, batteries and energy materials, ferroelectric materials, zeolite chemistry, negative thermal expansion, pharmaceutical polymorphism, and many others.

The most commonly cited disadvantage of powder diffraction is that the three-dimensional diffraction data of a single crystal is compressed onto the single dimension of the diffraction angle 2θ, meaning that different hkl reflections often overlap in 2θ. This overlap means that, in contrast to single crystal methods, it can be difficult or impossible to experimentally determine the accurate intensities of individual reflections needed for structural analysis. The solution to this problem is to adopt a whole-pattern fitting approach in which a structural model, a description of the peak shapes, and parameters to describe the background are used to calculate a powder pattern. The calculated intensity, $y_{\mathrm{calc},i}$, at each step in 2θ is then compared to the observed intensity $y_{\mathrm{obs},i}$, and the difference between the two is minimized by changing certain parameters of the model. This is most commonly done by a least-squares refinement in which the quantity minimized is

$$\sum_{i=1}^{N} w_i (y_{\mathrm{obs},i} - y_{\mathrm{calc},i})^2 \tag{14}$$

This is an iterative multistep process in which the model (hopefully) improves in each cycle of refinement and is used to initiate a subsequent minimization cycle. The process is normally followed by monitoring the weighted profile R factor, R_{wp}, which should tend to a low value

$$R_{\mathrm{wp}} = \sqrt{\frac{\sum_{i=1}^{N} w_i (y_{\mathrm{obs},i} - y_{\mathrm{calc},i})^2}{\sum_{i=1}^{N} w_i y_{\mathrm{obs},i}^{\ 2}}} \tag{15}$$

or a quantity such as goodness of fit (GoF) or χ, which relates R_{wp} to the statistically expected value R_{exp}

$$\mathrm{GoF} = \chi = \frac{R_{\mathrm{wp}}}{R_{\mathrm{exp}}} = \sqrt{\frac{\sum_{i=1}^{N} w_i (y_{\mathrm{obs},i} - y_{\mathrm{calc},i})^2}{N - P}} \tag{16}$$

where N is the number of data points and P the number of parameters. χ should tend to 1 for a good refinement. Least-squares uses a $1/\sigma(y_{\mathrm{obs},i})^2$ weighting, where $\sigma(y_{\mathrm{obs},i})$ is the experimental uncertainty in $y_{\mathrm{obs},i}$. A diffraction pattern recorded on a conventional powder diffractometer with a point detector will typically follow Poisson statistics such that $\sigma(y_{\mathrm{obs},i}) = \sqrt{y_{\mathrm{obs},i}}$; the resulting $1/y_{\mathrm{obs},i}$ weighting is assumed for all the powder diffraction examples in the paper.

Common parameters refined when fitting the data include structural parameters (the sample unit-cell parameters, fractional atomic coordinates, atomic site occupancies and atomic displacement parameters), parameters describing the instrument calibration (e.g., any 2θ zero-point offset), parameters describing any 2θ-dependent intensity correction (e.g., due to absorption), parameters describing the peak shape, and parameters describing the background between the Bragg peaks. The method was first coded by Hugo Rietveld and is usually referred to as Rietveld refinement.[35−38]

There are a few other important whole-pattern fitting methods used in powder diffraction analysis. One is to simply freely refine the 2θ values and intensities of peaks to describe each reflection without a structural model. This can be a good way to obtain peak 2θ positions, which can be used to determine unit-cell parameters in a process called auto-indexing. Problems can arise as a result of the large number of parameters when there is significant peak overlap. Another is to adjust the intensity of each reflection but at 2θ values constrained by a unit cell and hkl indices. This approach can substantially reduce the number of parameters relative to free peak fitting and lets you decide the best fit possible to an experimental data set for a given unit cell. Methods to achieve this are usually called Pawley or Le Bail fitting, and the differences in the underlying algorithms of the two methods are explained in the references.[24,39−41]

It is also worth noting that we need a starting structural model for Rietveld refinement in order to produce a reasonable initial calculated powder diffraction pattern. Structure solution is outside the main scope of this paper, but we could use the peak intensities from whole-profile fitting and single-crystal-like methods (e.g., direct methods, charge flipping) to come up with a structural model.[42] Alternatively, there are a variety of methods now available for rapidly testing computer-generated guessed structures against experimental data to find a plausible starting model;[42] students can explore this in the final part of Section 6. However, the most common approach is to use an approximate structural model derived from a related compound.

4. INTRODUCTION TO LEAST-SQUARES FITTING

We normally have students start with a simple artificial example of model fitting, but one which illustrates the general approach and teaches some important pitfalls. Let us take the first two columns in Table 1 from a simple "experiment" and plot the data (Figure 3a, blue points). The values could represent the number of flowers on a rose bush on a given day. If we wanted a simple model to predict the number of flowers on day 5, we could fit a linear expression $y = mx + c$ to obtain the gradient ($m = 5.3$) and intercept ($c = -4.5$) allowing us to predict the number of flowers on day 5 as 22. In Excel, the

Table 1. Data Values for Least-Squares Fitting

Day	Number of Flowers	Day	Number of Flowers
1.0	2	0.0	1.5
2.0	5	0.5	1
3.0	10	1.5	3
4.0	18	2.5	8
		3.5	13
		4.5	21
		5.0	25

https://dx.doi.org/10.1021/acs.jchemed.0c01016
J. Chem. Educ. 2021, 98, 495−505

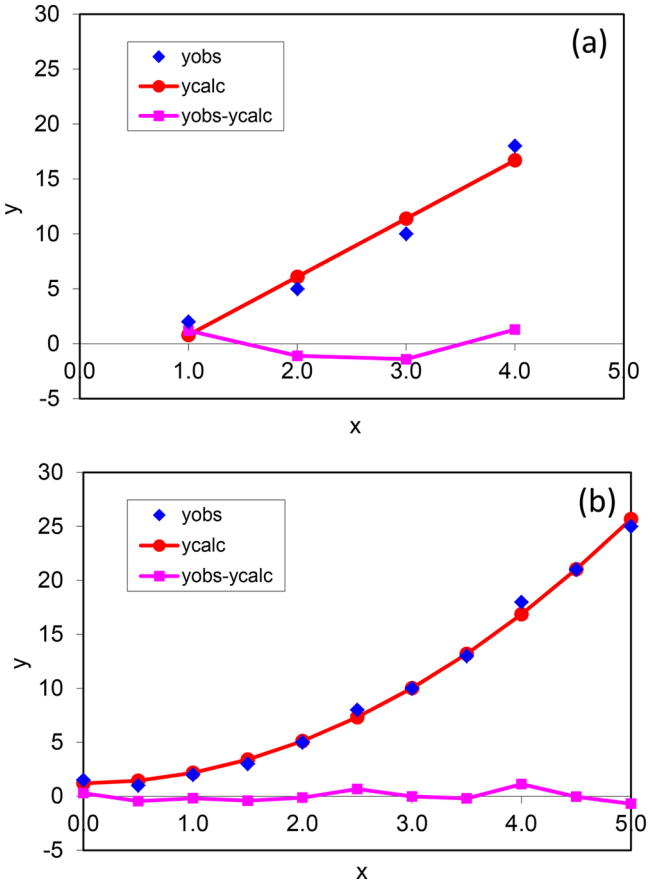

Figure 3. Fitting simple (a) linear and (b) polynomial functions in Excel.

normal approach would be to "right click on plot, add trendline". What Excel is actually doing here is minimizing $\sum_i (y_{obs,i} - y_{calc,i})^2$ for all data points by adjusting or refining the values of m and c in a process called least-squares refinement. In other words, it minimizes eq 14 under the assumption of equal weights for each experimental observation.

As illustrated in the accompanying Excel spreadsheet, students can do the same thing more explicitly in Excel using its built-in Solver routine. In the spreadsheet *solver_linear_fit*, they can define values for m and c in individual cells. For each value of x they can create columns containing y_{obs}, y_{calc} $(=mx + c)$, $(y_{obs} - y_{calc})$, and $(y_{obs} - y_{calc})^2$. They can create a cell containing the sum of the $(y_{obs} - y_{calc})^2$ column [or use the Excel SUMSQ function on $(y_{obs} - y_{calc})$], and use Solver to minimize this cell by varying the cells containing m and c. This gives values of $m = 5.3$ and $c = -4.5$, identical to the simple "add trendline" approach. An annotated spreadsheet containing all the equations in Excel format and full student-facing instructions are included in the Supporting Information.

With this linear example, it is also straightforward (but a little tedious) for students to do the least-squares analysis by hand using simple matrix mathematics. This also lets them calculate the standard uncertainties on the refined parameters and the correlations between them. We find that students enjoy doing this exercise once in their lives but rapidly realize why computers are generally used! This exercise is outlined in the Supporting Information. The answers can be checked in Excel using its built-in linear least-squares array function "LINEST"; details on how to do this are again provided in the spreadsheet *solver_linear_fit*.

Figure 3b is a plot containing all of the data values contained in Table 1 and shows that the analysis just performed (using only a subset of the data) was rather naïve. If we look at the full data set, where there are more observations collected over a larger x range, we see that a simple straight line fit is not appropriate. However, students can easily modify the Excel spreadsheet and try fitting the data to an expression such as $y = mx^2 + c$. This gives a much better fit. Note that at the end of this good least-squares fit the difference curve (pink) is scattered randomly around zero.

We find it useful to discuss the learning outcomes of this section with students. Some of these follow:

1. Excel can be used to fit arbitrary nonlinear functions to experimental data.
2. When performing data analysis, derived results are only reliable with an appropriate model.
3. Collecting data over as wide a set of conditions (here x values) as possible is important for testing the reliability of a given model. Later, students can explore the somewhat analogous problem of, for example, trying to simultaneously refine atomic displacement parameters and site occupancies in a Rietveld refinement over a limited 2θ range.
4. In a real analysis, one would ideally have experimental uncertainties associated with each observation such that the statistical reliability of different models can be assessed.

5. FITTING GAUSSIAN AND LORENTZIAN PEAK SHAPES

Many analytical techniques give rise to signals recorded as peaks which can be described using either Gaussian or Lorentzian functions (eqs 11 and 12, respectively). Early low-resolution neutron powder diffractometers gave essentially Gaussian peaks. Most X-ray powder diffractometers give peak shapes that can described by a mixture of Gaussian and Lorentzian functions, with the Lorentzian contribution often dominating.

The Excel sheet *solver_fit_gaussian* contains a simulated "experimental" data set which consists of a Gaussian function of intensity 500 units, *fwhm* 0.3 centered at $x = 3.0$, with a small nonzero background and artificial experimental noise. On the basis of their learning from Section 4, students can use eq 11, the variable parameters ($pos \equiv 2\theta_{hkl}$, *int*, *fwhm*) to fit the peak, and a 2θ-dependent polynomial to fit the background. Instructions are given in the Excel sheet *solver_fit_gaussian*, and in a TA/Instructor-focused format in the Supporting Information. An ideal fit is shown in Figure 4a.

Once they have a starting model, students should try starting values (*pos*, *int*, *fwhm* = 2.5, 200, 0.3) and use the Solver function to minimize $\sum_i (y_{obs,i} - y_{calc,i})^2$ to fit the observed data. They should find the sum reduces rapidly from $\sim 3 \times 10^7$ ($R_{wp} \approx 106\%$) to 2.8×10^4 ($R_{wp} = 3.2\%$) in around 10 cycles. The minimization process can be followed in the bottom left of the Excel window. If they enable "Show Iteration Results" in the Solver options, they can follow each least-squares cycle graphically. The final fit should give (*pos*, *int*, *fwhm* = 3.0, 497, 0.3), and the difference curve should be randomly scattered around zero (Figure 4a). Note that students might get slightly different R_{wp} values with different models, if their

https://dx.doi.org/10.1021/acs.jchemed.0c01016
J. Chem. Educ. 2021, 98, 495−505

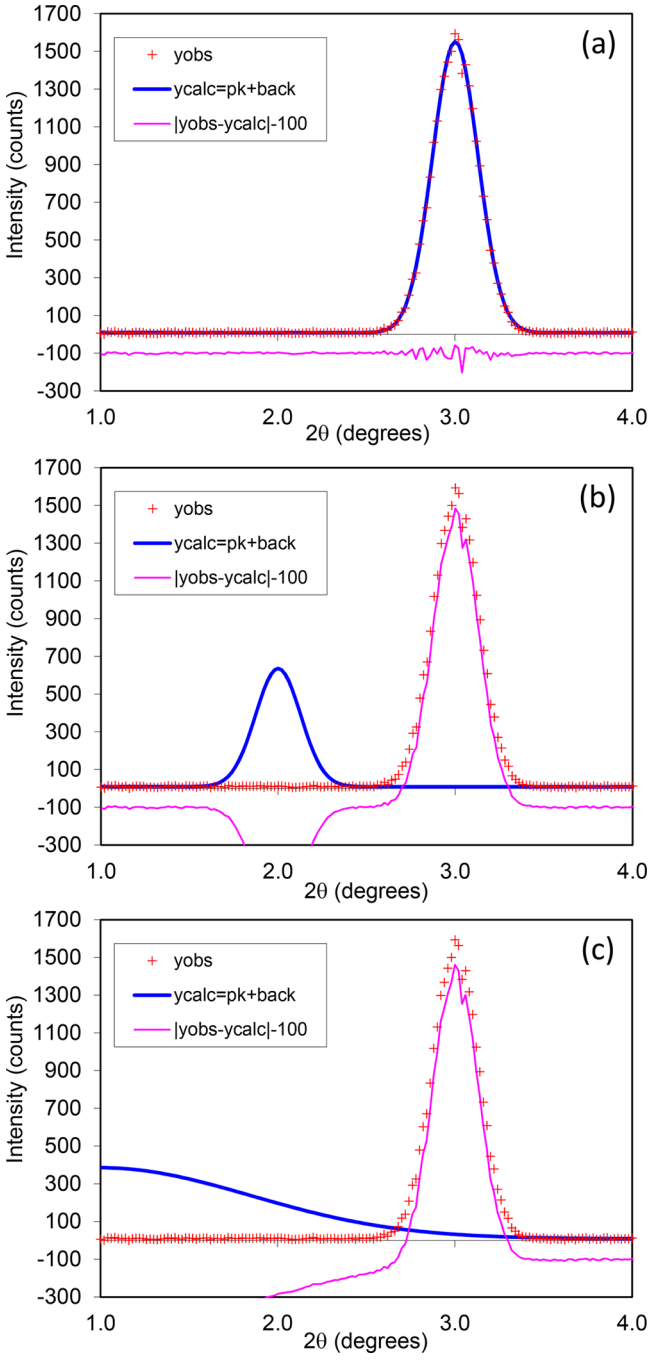

Figure 4. Fitting a Gaussian function in Excel: (a) the converged fit, (b) (*pos*, *int*, *fwhm* = 2.0, 200, 0.3), which does not converge, and (c) (*pos*, *int*, *fwhm* = 1.0, 800, 2.0), which does converge.

refinements are not fully converged or, potentially, with different Excel versions.

We use this example to let students test some of the convergence properties of least-squares fitting, that is, how close the starting model needs to be for it to converge to the lowest R_{wp} minimum. This teaches how a "good model" can sometimes fail to converge to fit the data, whereas a "bad model" will converge. For example, Figure 4b,c shows starting models with (b) (*pos*, *int*, *fwhm* = 2.0, 200, 0.3), R_{wp} = 107%, and (c) (*pos*, *int*, *fwhm* = 1.0, 800, 2.0), R_{wp} = 114%. Students should find that, despite the starting model in panel c being (visually and based on R_{wp}) a "worse starting model" than in panel b, it will reliably converge. We ask students to test different starting models to come up with a criterion for reliable convergence. The simple observation in this case is that there needs to be some overlap between the obs and calc peaks. In other words, models like Figure 4b will generally diverge, but those like Figure 4c will converge as the blue line crosses the experimentally observed peak. Even a "terrible" starting model such as (*pos*, *int*, *fwhm* = 0.5, 2000, 10.0) will usually converge if it meets this criterion, whereas seemingly more reasonable models will not. This helps students appreciate why it is important to think about the best starting parameters to use in least-squares analysis; small manual adjustments are often needed before "blind" refinement. Later on (Section 6), they realize these ideas are crucial in performing a successful Rietveld refinement.

Students could be asked to set up a similar sheet to fit a Lorentzian function (eq 12). A model answer is given in sheet *fit_lorentzian_answer*. They should see that the best-fit Lorentzian is, as expected, significantly worse than the best-fit Gaussian. Students should also see that an *int* = 500 Lorentzian is narrower at its half height than a Gaussian but has wider "tails".

Peaks in a laboratory powder X-ray pattern are usually described well with a mixture of Gaussian and Lorentzian functions. One approach is to use the pseudo-Voigt formulation given in eq 13 that contains a mixing parameter η ($0 \leq \eta \leq 1$). Students can explore this in spreadsheet *fit_pv_answer* which uses a single peak from the X-ray diffraction pattern of TiO_2 discussed below and lets the student try fitting a Gaussian (G), a Lorentzian (L), or an $\eta G + (1 - \eta)L$ pseudo-Voigt. This particular example fits well with $\eta \approx 0.5$. As Lorentzian broadening often dominates in many powder diffractometers, we use Lorentzian functions exclusively in later analysis.

6. WHOLE-POWDER-PATTERN FITTING: PEAKS, PAWLEY/LE BAIL, AND RIETVELD REFINEMENT

With the basic ideas of peak fitting understood, students can explore whole-powder-pattern fitting methods. They do this initially using a simulated powder diffraction pattern of TiO_2 so there are no issues caused by any systematic errors in a real data set. The simulation means that atomic displacement parameters can be ignored (B = 0 in eq 9), and that they can use a constant background of ~26 counts in the analysis and $1/y_{obs,i}$ weighting. We use a Lorentzian peak shape for simplicity.

Sheet *TiO2_pkfit* and the accompanying student questions explore how the powder pattern from 10−42° can be fitted by summing four individual peaks of the type used in Section 5 and a simple background function (here a constant). By refining 13 parameters [a single background coefficient, and 3 × (*pos*, *int*, *fwhm*) for the four reflections], students can get a good fit to the data with R_{wp} = 17.2%. This is a good approach for extracting precise peak positions and intensities when peaks do not overlap. In this and later spreadsheets, the fit to the experimental data is presented graphically using a conventional "Rietveld plot" style. Observed data are shown as red points, the calculated pattern as a solid blue line, and the difference as an offset pink line. The $2\theta_{hkl}$ values of each reflection are marked with a small triangle. It is worth noting that our fitting approach is computationally somewhat wasteful in that each peak is summed over the entire 2θ range. In most specialized Rietveld refinement software, the 2θ range over which a peak

https://dx.doi.org/10.1021/acs.jchemed.0c01016
J. Chem. Educ. 2021, 98, 495−505

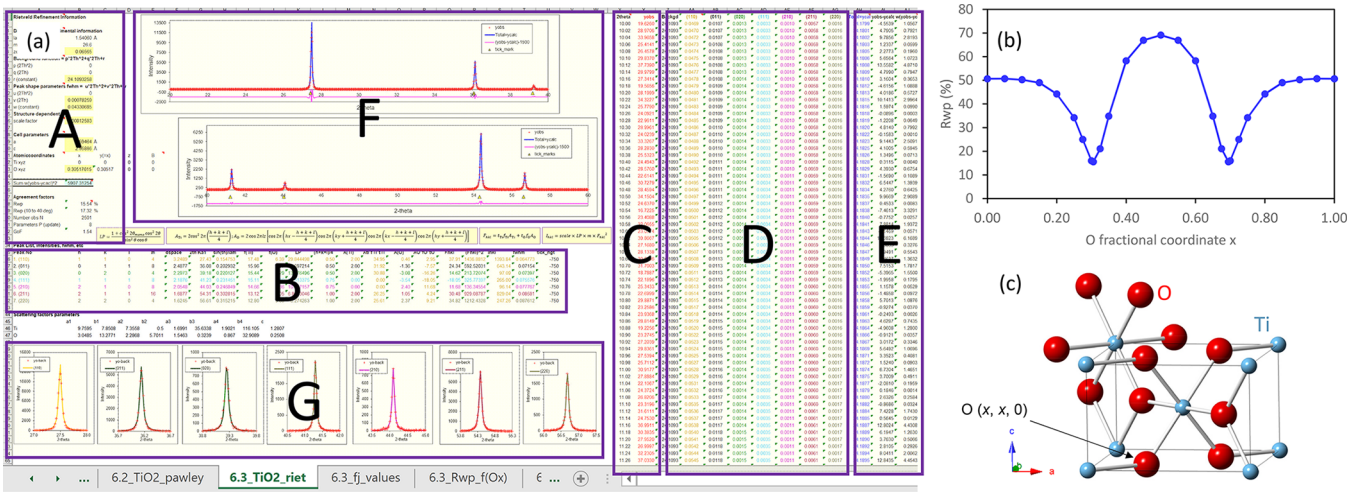

Figure 5. (a) Excel spreadsheet used for Rietveld refinement, with annotated sections discussed in the text. (b) Dependence of R_{wp} on fractional atomic coordinate x of O on site (x, x, 0). (c) The rutile structure (Ti blue, oxygen red), with oxygen sites in neighboring unit cells included to show the coordination sphere around a Ti on one cell corner.

contributes is limited to a narrower region close to $2\theta_{hkl}$ for speed. Rietveld-specific software would, of course, also perform many of the calculations using loops, which leads to a much more compact description than our Excel approach.

Sheet *TiO2_pawley* moves students one step closer to a Rietveld refinement. Here, the peak intensities and widths are allowed to refine freely, but the peak positions are calculated from the unit-cell parameters via eqs 1 and 2 and a parameter to describe any peak offset. This is defined as a zero-point calibration ($2\theta_{true} = 2\theta_{obs} -$ zero), but in real experiments could be correcting for a minor error in mounted sample height. We plot the *hkl* tick marks at the $2\theta_{true}$ position. Students can now refine the unit-cell parameters directly from the experimental data. The intensities (with eq 5 corrections) could be used for either quantitative analysis in a multiphase sample, or to attempt structure solution. Note that we obtain R_{wp} = 17.2% in this example, identical to that for the free peak fitting approach, despite using one fitting parameter fewer. We typically set students a challenge problem of modifying the spreadsheet so that peak *fwhm*'s show a smooth 2θ dependence, further reducing the number of fitting parameters.

Sheet *TiO2_riet* takes students all the way to a full Rietveld structural analysis. We will discuss it in some detail with reference to the annotated sheet in Figure 5a. Section A in this figure contains the parameters which are needed in the model. The diffractometer-related information includes the wavelength and monochromator angle (needed for the LP correction, eq 10). Parameters p, q, and r are used to describe a 2θ-dependent background polynomial (we continue using just term r). Parameters u, v, and w are used to describe a simple empirical 2θ-dependent peak fwhm. An overall scale factor is specified. Finally, the structural information is given in terms of unit-cell parameters a and c and the fractional atomic coordinates and displacement parameters (B) of each atom in the asymmetric unit.

Section B in in Figure 5a contains the calculations that determine the position and intensity of each reflection. These replace the freely refined values in earlier spreadsheets. Peak positions in degrees 2θ are calculated from the h, k, and l Miller indices, cell parameters, and wavelength using Bragg's law. The atomic scattering factors f_{Ti} and f_O are then calculated at this sin θ/λ value based on the parameters reported in the International Tables Volume C[43] and ignore anomalous scattering[24] (these are also plotted for the student in sheet *fj_values*). The LP correction and structure factor F_{hkl} are then calculated for each reflection. Equation 5 is used to calculate I_{hkl}, and the fwhm is calculated from u, v, w, and $2\theta_{hkl}$.

As with the least-squares by-hand exercise in Section 4, we find that it is instructive for students to calculate the I_{hkl} peak intensity for at least one reflection in this simple example "by-hand". This helps them engage and understand the equations and correction factors that feed into everyday crystallographic calculations. It, again, also teaches them why prewritten crystallography software is so convenient! This exercise is in the Supporting Information.

Section C in Figure 5a contains the experimental data as columns of 2θ and y_{obs}, and Section D calculates the powder pattern. This is equivalent to the earlier examples and contains a Lorentzian peak for each *hkl* reflection with the position (plus any $2\theta_{zero}$ correction), intensity, and fwhm calculated in Section B. Each *hkl* row/column combination of Sections B and D is color-matched for clarity. The overall y_{obs} is then calculated in Section E by summing each peak with the background function, and the values of $(y_{obs} - y_{calc})$ and $w(y_{obs} - y_{calc})^2$ calculated.

The bottom of Section A contains the sum of the $w(y_{obs} - y_{calc})^2$ column and should be minimized to perform a Rietveld refinement. This cell is shaded blue, and the parameters that might be refined are shaded yellow. The final Sections F and G show the conventional Rietveld plots of observed, calculated, and difference patterns for the whole data set, and magnified views of the seven individual *hkl* reflections.

We typically present the spreadsheet to students in the "fully refined" state, with R_{wp} = 15.5%, though instructors might want to present a more approximate starting model so that students have to make refinement choices. These two possibilities are stored in Excel's "Data/What-If Analysis/Scenario Manager" as two different scenarios. We have included a suggested set of questions that students could explore in the Supporting Information. These are deliberately set as challenge problems for students and explore topics such as the following.

- How does each individual parameter change the calculated pattern? How sensitive is the refinement to

https://dx.doi.org/10.1021/acs.jchemed.0c01016
J. Chem. Educ. 2021, 98, 495−505

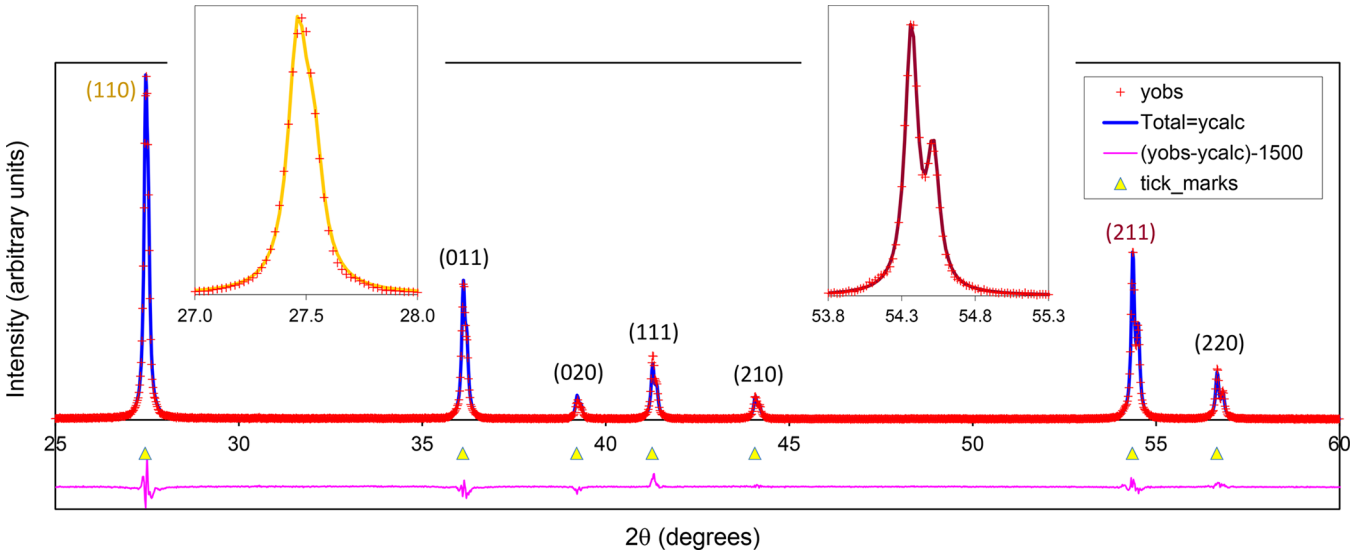

Figure 6. Rietveld fit to experimental data discussed in Section 7. Observed data shown as red crosses, calculated as a solid blue line, and the difference curve (offset) as a pink line. Arrows show the predicted 2θ values of different *hkl* reflections. Insets show zooms of the (110) and (211) reflections. Note how the Kα1/α2 radiation leads to clear peak splitting at higher 2θ.

different parameters? How much can parameters be changed before the refinement no longer converges to the global minimum? When will a Rietveld refinement get "stuck" in a false minimum? Is there more than one model that can fit the experimental data? Students are encouraged to generate plots such as Figure 5b, which shows the dependence of R_{wp} on the oxygen fractional atomic coordinate.

- How sensitive are the important structural parameters to inadequacies in other aspects of the model? Which parameters are highly (or infinitely) correlated in a crystallographic refinement and potentially unreliable?
- How can the spreadsheet be adapted to fit either neutron powder diffraction data or single crystal diffraction data? What are the pros and cons of these different experiments?
- What structural information can be deduced from the Rietveld fit? What are the bond lengths and bond angles in the refined structural model? What is the connectivity pattern of the TiO_6 octahedra? How does the structure help explain the high electronic conductivity of analogues like VO_2, and how might diffraction data be used to reveal structural changes when VO_2 undergoes a metal to insulator transition on cooling?
- Finally, we stated early in the paper that, while the Rietveld method is generally used for structure refinement rather than structure solution, it is possible to solve structures *ab initio* from powder data. Students are encouraged to explore how Excel can be used to start refinements from different random starting models and essentially solve the crystal structure from scratch. While this is a trivial example, remarkably complex unknown structures have been solved with this type of approach.[25,44−46]

Students should also be asked to consider the reliability of the Rietveld structural fit. The most important indicator of the correctness of a Rietveld fit is the visual inspection of the match between the calculated and observed patterns.[25] All observed reflections should be explained by the model and their relative intensities correctly described. No unfitted extra reflections should be observed. As students explore in Supporting Information problem 6.6, minor features in the difference curve due to the approximate peak shape model can usually be ignored, provided the over- and undercalculated areas are comparable. It is difficult to make quantitative conclusions on the uncertainty in the refined O *x* coordinate as the peak shape issues lead to correlated $(y_{obs} - y_{calc})$ residuals. As such, the Rietveld-derived standard uncertainty (here ~0.0005) is almost certainly an underestimate of the true uncertainty.[25] However, the shape of an R_{wp} plot like that of Figure 5b, and the sensible geometry of the Rietveld-derived structure, gives confidence in the model's reliability.

Students should also consider the fact that this exercise was limited to the first seven peaks in the powder diffraction to keep the spreadsheet manageable. In a normal Rietveld analysis, one would analyze data to a higher 2θ, thus including many more *hkl* reflections. This would improve the reliability of the derived parameters and help reduce correlations between parameters which give different I_{hkl} dependencies on 2θ (e.g., site occupancies give no direct 2θ dependence, temperature factors do via eq 9). This is somewhat analogous to Figure 3a,b, where the wider *x* range in Figure 3b clearly showed that a nonlinear model is required.

Students going on to perform Rietveld refinement as part of their research might want to analyze the same data set in one of the mainstream Rietveld software packages. The Supporting Information contains the files needed to perform equivalent Rietveld analysis in TOPAS or GSAS-1.[34,47−50]

7. RIETVELD REFINEMENT WITH REAL EXPERIMENTAL DATA

Sheet *TiO2_riet_real_data* takes the analysis one step further and engages students with real experimental data. Students can use this sheet to analyze data collected on a typical laboratory instrument. The example data set provided was collected in ~30 min on a Siemens d5000 diffractometer with a pyrolytic graphite diffracted beam monochromator and point detector (i.e., a very much non-state-of-the-art instrument). The

https://dx.doi.org/10.1021/acs.jchemed.0c01016
J. Chem. Educ. 2021, 98, 495−505

experimental setup introduces one additional complication in that the X-ray tube produces a mixture of Cu Kα1 and Kα2 radiation with wavelengths of 1.5406/1.5445 Å that reach the detector in a ~ 2:1 ratio.[51] This means that a pair of closely spaced peaks are observed for each *hkl* reflection in the powder diffraction pattern. This is treated in the sheet *TiO2_riet_real_data* by summing a second Lorentzian peak, with intensity scaled by the value of $K_{ratio} = 0.5$, at position $2\theta_{hkl}$ for Kα2 radiation. Scattering factors and intensity corrections are assumed to be unchanged relative to Kα1 radiation.

Students can perform an analysis similar to that described in Section 6 on either the experimental data set provided, or an equivalent data set of their own collected as part of a laboratory practical. Pop-up comments on the various spreadsheet cells suggest sensible instrumental parameter values for other common experimental setups. A typical final Rietveld plot is shown in Figure 6. Student exercises which explore the experimentally derived structure and discuss its relevance to understanding physical properties are given in the Supporting Information.

8. CLASSROOM EXPERIENCE AND ANALYSIS OF EFFECTIVENESS

The Excel Rietveld spreadsheet was originally developed for a biennial international graduate student training school that the authors have co-run with colleagues from the ESRF and UCL since 2004. Students in the five-day residential school come from a wide range of disciplines (chemistry, archeology, earth sciences, engineering, materials, pharmacy, physics, industry, etc.) with very different backgrounds and prior training. In the earliest schools, we taught using a traditional combination of formal lectures and detailed "how to do this refinement" exercises in common Rietveld packages. Our experience was that even by the end of the school many students had little understanding of the physical meaning of different "tick box" parameters used in data fitting. This reflects a lack of deep or critical learning and leaves students unable to tackle new or more challenging problems. We now adopt a teaching model which involves relatively concise content delivery through lectures or reading (~25% of time), time (~25%) for students to undertake by-hand problem solving exercises working in small groups, and ~50% of time working in a computer lab, a time-on-task focus. The material described in this article is one of the early computer exercises and has been completed by over 400 students. Given the very different backgrounds of the students, we let them work through the exercises independently at their own speed. We staff the computer lab with ~1 TA per 12 students, and TA time ends up roughly evenly split between giving specific how-to guidance to the less experienced students and setting/discussing challenge problems with those more experienced. In this environment, we make no attempt to assess students in a traditional "did they get the right answer and complete all the problems" sense. We also encourage them to set their own goals. For some students, performing an independent fit to a single Gaussian peak (Section 5) is as valuable as exploring all the aspects of Rietveld analysis in a real experimental data set (Section 7) is to others.

Our emphasis when discussing the exercise with the class is the bottom-up approach of building up ideas and complexity (Figure 1). For example, Section 4 starts students with the basics of linear least-squares fitting and sets a challenge of fitting arbitrary nonlinear functions; Section 5 introduces a peak shape function and sets a student challenge to also add in a function to describe the experimental background. Section 6 (sheets 6.1 and 6.2) generalizes to multiple peaks, with a student challenge to describe smoothly varying peak shapes; sheet 6.3 finally combines all the ideas into a full Rietveld fit. Students also identify issues associated with inappropriate models or fitting approaches in early simple examples, which they can reapply in the more complex Rietveld examples. We find that the common question of "Why didn't this refinement work?" when students later attempt much more complex refinements can usually be answered with a response such as "Think back to exercise 5.2, why didn't that work?". While it would be possible to work through these ideas in other software packages or in specialist Rietveld software, we chose Excel as the one package that almost all students are familiar with, and that they can almost certainly access. We have lost count of the number of times students have said "I didn't know Excel could do this", or the number who have said they can now see how to apply similar approaches to analyze other data.

Our assessment of the effectiveness of the approach is judged via pre- and postcourse questionnaires to assess the background and confidence levels of students before the school against their experiences of the different teaching activities. The residential nature of the school also means we can discuss learning informally during meal breaks and nonacademic sessions. Student feedback is uniformly that the experience of working through a complex data analysis problem from scratch helps cement fundamental ideas and identifies knowledge gaps that they might otherwise skip over. Students comment explicitly that the Excel-based exercises lead to a better understanding of what Rietveld software packages do and nurture a more critical approach to their use.

While we have used these exercises primarily with undergraduate and postgraduate research students, they could readily form part of a senior-level practical experiment or an inquiry-based miniproject. This would give students the experience of working all the way from an analytical measurement through to a quantitative three-dimensional structural model. This will, *inter alia*, help them appreciate the origin of much of the information they learn about interatomic bond distances and coordination geometry, which is so fundamental to chemistry and other disciplines. Even for students not likely to perform powder diffraction or crystallographic analysis later in their careers, the data analysis philosophy taught is widely reapplicable. The Excel exercises described here are also mirrored in separate online tutorials using Rietveld-specific refinement software.[52] These allow students continuing to work with powder diffraction data to build from this specific simple example to much more challenging problems. Our website provides over 100 such problems for students to explore.[52]

9. CONCLUSIONS

In conclusion, we believe that the self-guided exploratory study program set out in this paper allows a student with no prior knowledge of data analysis, no computer-coding expertise, and only a basic background in crystallography to reach the point where they can perform a full structural analysis on a compound from scratch. For most students, this will be the first time they fully understand how the beautiful structural models drawn in their textbooks are derived. While the process is necessarily reasonably involved, we find that it is well within the capability of undergraduate students. The bottom-up

https://dx.doi.org/10.1021/acs.jchemed.0c01016
J. Chem. Educ. 2021, 98, 495−505

approach adopted allows students to test ideas on simple examples, which are later reapplied as the complexity of the problem necessarily increases. We believe that this experiential learning leads to much better student understanding than other approaches.[53] The ideas we explore are widely reapplicable in other areas of data analysis.

■ ASSOCIATED CONTENT

Supporting Information

The Supporting Information is available at https://pubs.acs.org/doi/10.1021/acs.jchemed.0c01016.

Excel spreadsheet containing all the examples discussed in the paper (XLSX)

TOPAS and GSAS format files allowing analysis of the same data set used here in Rietveld-specific software (ZIP)

Student exercises to do linear regression by hand and to calculate the intensity of the (020) reflection of TiO_2; instructor notes on the spreadsheet contents; instructor notes containing specific student exercises for a computer lab, challenge problems, and discussion points; detailed instructions and annotated spreadsheet on linear function fitting for students with no previous experience in using Excel's Solver function; and simulated neutron powder diffraction pattern of TiO_2 (PDF, DOCX)

■ AUTHOR INFORMATION

Corresponding Author

John S. O. Evans − *Department of Chemistry, Durham University, Durham DH1 3LE, United Kingdom;* orcid.org/0000-0001-6305-6341; Email: john.evans@durham.ac.uk

Author

Ivana Radosavljevic Evans − *Department of Chemistry, Durham University, Durham DH1 3LE, United Kingdom;* orcid.org/0000-0002-0325-7229

Complete contact information is available at: https://pubs.acs.org/10.1021/acs.jchemed.0c01016

Notes

The authors declare no competing financial interest.

■ ACKNOWLEDGMENTS

We thank the generations of students who have attended the Durham Powder Diffraction and Rietveld Refinement school for extensive testing (and occasional breaking) of the Excel spreadsheet presented, and Andy Fitch (European Synchrotron Radiation Facility, ESRF), Jeremy Cockcroft (University College London, UCL), and many school tutors for feedback on their experiences using it as a teaching tool. We thank the Powder Diffraction Commission of the IUCr, Durham University, and Bruker for ongoing support of the school and EPSRC and Panalytical for supporting early schools.

■ REFERENCES

(1) Taylor, R.; Wood, P. A. A Million Crystal Structures: The Whole Is Greater than the Sum of Its Parts. *Chem. Rev.* **2019**, *119*, 9427−9477.

(2) Inorganic Crystal Sructure Database—ICSD. https://icsd.products.fiz-karlsruhe.de/ (accessed November 2020).

(3) International Centre for Diffraction Data PDF. https://www.icdd.com/ (accessed November 2020).

(4) Sojka, Z.; Che, M. Presentation and Impact of Experimental Techniques in Chemistry. *J. Chem. Educ.* **2008**, *85* (7), 934−940.

(5) Hoggard, P. E. Integrating Single Crystal X-Ray Diffraction in the Undergraduate Curriculum. *J. Chem. Educ.* **2002**, *79* (4), 420−421.

(6) Hulien, M. L.; Lekse, J. W.; Rosmus, K. A.; Devlin, K. P.; Glenn, J. R.; Wisneski, S. D.; Wildfong, P.; Lake, C. H.; MacNeil, J. H.; Aitken, J. A. An Inquiry-Based Project Focused on the X-ray Powder Diffraction Analysis of Common Household Solids. *J. Chem. Educ.* **2015**, *92* (12), 2152−2156.

(7) Battle, G. M.; Ferrence, G. M.; Allen, F. H. Applications of the Cambridge Structural Database in Chemical Education. *J. Appl. Crystallogr.* **2010**, *43* (5 Part 2), 1208−1223.

(8) Grazulis, S.; Sarjeant, A. A.; Moeck, P.; Stone-Sundberg, J.; Snyder, T. J.; Kaminsky, W.; Oliver, A. G.; Stern, C. L.; Dawe, L. N.; Rychkov, D. A.; Losev, E. A.; Boldyreva, E. V.; Tanski, J. M.; Bernstein, J.; Rabeh, W. M.; Kantardjieff, K. A. Crystallographic Education in the 21st Century. *J. Appl. Crystallogr.* **2015**, *48* (6), 1964−1975.

(9) Pett, V. Teaching Crystallography to Undergraduate Physical Chemistry Students. *J. Appl. Crystallogr.* **2010**, *43*, 1139−1143.

(10) Kantardjieff, K. A.; Kaysser-Pyzalla, A. R.; Spadon, P. Crystallography Education and Training for the 21st Century. *J. Appl. Crystallogr.* **2010**, *43*, 1137−1138.

(11) Toby, B. H. Observations on Online Educational Materials for Powder Diffraction Crystallography Software. *J. Appl. Crystallogr.* **2010**, *43*, 1271−1275.

(12) Brannon, J. P.; Ramirez, I.; Williams, D.; Barding, G. A.; Liu, Y.; McCulloch, K. M.; Chandrasekaran, P.; Stieber, S. C. E. Teaching Crystallography by Determining Small Molecule Structures and 3-D Printing: An Inorganic Chemistry Laboratory Module. *J. Chem. Educ.* **2020**, *97* (8), 2273−2279.

(13) Zheng, S.-L.; Campbell, M. G. Connecting Key Concepts with Student Experience: Introducing Small-Molecule Crystallography to Chemistry Undergraduates Using a Flexible Laboratory Module. *J. Chem. Educ.* **2018**, *95* (12), 2279−2283.

(14) Campbell, M. G.; Powers, T. M.; Zheng, S.-L. Teaching with the Case Study Method To Promote Active Learning in a Small Molecule Crystallography Course for Chemistry Students. *J. Chem. Educ.* **2016**, *93* (2), 270−274.

(15) Wilson, C. C.; Parkin, A.; Thomas, L. H. Frontiers of Crystallography: A Project-Based Research-Led Learning Exercise. *J. Chem. Educ.* **2012**, *89* (1), 34−37.

(16) Rosenthal, J. Spreadsheet Calculations for X-ray powder Diffraction Patterns. *J. Chem. Educ.* **1991**, *68* (11), A285−A286.

(17) Stojilovic, N.; Isaacs, D. E. Inquiry-Based Experiment with Powder XRD and FeS2 Crystal: "Discovering" the (400) Peak. *J. Chem. Educ.* **2019**, *96* (7), 1449−1452.

(18) Corsepius, N. C.; DeVore, T. C.; Reisner, B. A.; Warnaar, D. L. Using Variable Temperature Powder X-ray Diffraction To Determine the Thermal Expansion Coefficient of Solid MgO. *J. Chem. Educ.* **2007**, *84* (5), 818−821.

(19) Longo, E.; Espinosa, J. W. M.; Souza, A. G.; Lima, R. C.; Paris, E. C.; Leite, E. R. Structural Order−Disorder Transformations Monitored by X-ray Diffraction and Photoluminescence. *J. Chem. Educ.* **2007**, *84* (5), 814−817.

(20) Varberg, T. D.; Skakuj, K. X-ray Diffraction of Intermetallic Compounds: A Physical Chemistry Laboratory Experiment. *J. Chem. Educ.* **2015**, *92* (6), 1095−1097.

(21) Ismail, M. N. Hydrothermal Synthesis and Characterization of Titanosilicate ETS-10: Preparation for Research Integrated Inorganic Chemistry Laboratory Course. *J. Chem. Educ.* **2020**, *97* (6), 1588−1594.

(22) Pires, J. Simple Analysis of Historical Lime Mortars. *J. Chem. Educ.* **2015**, *92* (3), 521−523.

(23) Martín-Ramos, P.; Susano, M.; Gil, F. P. S. C.; Pereira da Silva, P. S.; Martín-Gil, J.; Silva, M. R. Facile Synthesis of Three Kobolds: Introducing Students to the Structure of Pigments and Their Characterization. *J. Chem. Educ.* **2018**, *95* (8), 1340−1344.
(24) Dinnebier, R. E.; Leineweber, A.; Evans, J. S. O. *Rietveld Refinement, Practical Powder Diffraction Pattern Analysis using TOPAS*; De Gruyter, 2018; p 331.
(25) McCusker, L.; Von Dreele, R.; Cox, D.; Louër, D.; Scardi, P. Rietveld Refinement Guidelines. *J. Appl. Crystallogr.* **1999**, *32* (1), 36−50.
(26) Young, R. A. *The Rietveld Method*; Oxford University Press, 1993.
(27) Matching online tutorials. http://community.dur.ac.uk/john.evans/topas_workshop/tutorial_riet_excel.htm (accessed November 2020).
(28) Blake, A. J.; Cole, J. M.; Evans, J. S. O.; Main, P.; Parsons, S.; Watkin, D. J. *Crystal Structure Analysis: Principles and Practice*; Oxford University Press, 2009.
(29) Clegg, W. *Crystal Structure Determination*; Oxford University Press, 1998.
(30) Giacovazzo, C.; Monaco, H. L.; Viterbo, D.; Scordari, F.; Gilli, G.; Zanotti, G.; Catti, M. *Fundamentals of Crystallography*; Oxford University Press, 2002.
(31) *International Tables for X-Ray Crystallography, Vol. I Symmetry Groups*; Kynoch Press, 1969.
(32) Evans, J. S. O.; Evans, I. R. Beyond Classical Applications of Powder Diffraction. *Chem. Soc. Rev.* **2004**, *33* (8), 539−547.
(33) Pecharsky, V.; Zavalij, P. *Fundamentals of Powder Diffraction and Structural Characterization of Materials*; Springer Science & Business Media, 2008.
(34) Dinnebier, R. E.; Billinge, S. J. *Powder Diffraction: Theory and Practice*; Royal Society of Chemistry, 2008; p 574.
(35) Rietveld, H. M. Line Profiles of Neutron Powder-Diffraction Peaks for Structure Refinement. *Acta Crystallogr.* **1967**, *22* (1), 151−152.
(36) Rietveld, H. M. A Profile Refinement Method for Nuclear and Magnetic Structures. *J. Appl. Crystallogr.* **1969**, *2* (2), 65−71.
(37) Rietveld, H. M. The Rietveld method. *Phys. Scr.* **2014**, *89* (9), 098002.
(38) van Laar, B.; Schenk, H. The Development of Powder Profile Refinement at the Reactor Centre Netherlands at Petten. *Acta Crystallogr., Sect. A: Found. Adv.* **2018**, *74* (2), 88−92.
(39) Le Bail, A. Whole Powder Pattern Decomposition Methods and Applications: A Retrospection. *Powder Diffr.* **2005**, *20* (4), 316−326.
(40) Le Bail, A.; Duroy, H.; Fourquet, J. Ab-initio Structure Determination of $LiSbWO_6$ by X-ray Powder Diffraction. *Mater. Res. Bull.* **1988**, *23* (3), 447−452.
(41) Pawley, G. Unit-cell Refinement from Powder Diffraction Scans. *J. Appl. Crystallogr.* **1981**, *14* (6), 357−361.
(42) David, W. I.; Shankland, K.; Baerlocher, C.; McCusker, L. *Structure Determination from Powder Diffraction Data*; Oxford University Press, 2002.
(43) Wilson, A. J. C. *International Tables for Crystallography. Vol. C: Mathematical, Physical and Chemical Tables*; Kluwer Academic Publishers (published for the International Union of Crystallography): Dordrecht, 1992; p 883.
(44) David, W. I. F.; Shankland, K. Structure determination from Powder Diffraction Data. *Acta Crystallogr., Sect. A: Found. Crystallogr.* **2008**, *64* (1), 52−64.
(45) Favre-Nicolin, V.; Cerny, R. FOX, 'Free Objects for Crystallography': a Modular Approach to Ab Initio Sstructure Determination from Powder Diffraction. *J. Appl. Crystallogr.* **2002**, *35* (6), 734−743.
(46) Harris, K. D., Powder Diffraction Crystallography of Molecular Solids. In *Advanced X-Ray Crystallography*; Springer, 2011; pp 133−177.
(47) Coelho, A. A. TOPAS and TOPAS-Academic: an Optimization Program Integrating Computer Algebra and Crystallographic Objects Written in C++. *J. Appl. Crystallogr.* **2018**, *51* (1), 210−218.
(48) Coelho, A. A.; Evans, J. S. O.; Evans, I. R.; Kern, A.; Parsons, S. The TOPAS Symbolic Computation System. *Powder Diffr.* **2011**, *26* (4), S22.
(49) Larson, A. C.; Von Dreele, R. B. *GSAS*; Los Alamos National Laboratory: Los Alamos, NM, 1994.
(50) Toby, B. H. EXPGUI, a Graphical User Interface for GSAS. *J. Appl. Crystallogr.* **2001**, *34* (2), 210−213.
(51) Stojilovic, N. Using Cu Kα1/Kα2 Splitting and a Powder XRD System To Discuss X-ray Generation. *J. Chem. Educ.* **2018**, *95* (4), 598−600.
(52) Online powder diffraction analysis tutorials. http://community.dur.ac.uk/john.evans/topas_workshop/tutorial_menu.htm (accessed November 2020).
(53) Svinicki, M. D.; McKeachie, W. J., Experiential Learning: Case-Based, Problem-Based and Reality-Based. In *McKeachie's Teaching Tips: Strategies, Research and Theory for College and University Teachers*, 14th ed.; Svinicki, M. D., McKeachie, W. J., Eds.; Wadsworth: Belmont, CA, 2015.

NOTE ADDED AFTER ASAP PUBLICATION

This paper was published ASAP on November 25, 2020, with a typographical error in an equation leading to the scattering factors in the Supporting Information Excel spreadsheet 6.3, though without effect on the values or conclusions in the paper. The corrected version was posted on January 12, 2021.

https://dx.doi.org/10.1021/acs.jchemed.0c01016
J. Chem. Educ. 2021, 98, 495−505